ISSN-XXXXXXXX (Online)

Shibli National Academic Journal

(A Six Monthly Multidisciplinary Multi Lingual Peer Reviewed Journal)

Chief Editor
Dr. Mohammad Zahid
www.snaj.org.in
chiefeditor@snaj.org.in

Shibli National Academic Journal **ISSN- XXXXXXX**
Vol. No. 1, Issue No. 1, Jan- Jun 2025

Scaling of Inverted PTB7-Th:PC7BM Organic Solar Cell for Large Area Organic Photovoltaic Modules

Dr Belal Usmani,

Abstract

Performance study of large area inverted organic photovoltaic (OPV) modules of configuration ITO/ZnO/PTB7-Th:$PC_{71}BM$/MoO_3/Ag are performed. At laboratory scale 0.06cm^2, this device configuration repeatedly demonstrates the power conversion efficiency (PCE) ~ 9 %, which is within the range of PCE normally achieved for this configuration. The OSMs with active area 9.25 cm^2 and 63 cm^2 are fabricated employing spin coating technique comprising total area 25 cm^2 (5cm x 5 cm) and 144 cm^2 (11cm x 11 cm), respectively. The 25 cm^2 modules, composed of 5 cells connected in series shows PCE 3.256%, with short-circuit current (J_{sc}), open circuit voltage (V_{oc}), and fill factor (FF), 3.210 $mAcm^{-2}$, 3.20 V, and 31.719 %. However, The 144 cm^2 modules, composed of 10 cells connected in series shows PCE 1.019, J_{sc}, V_{oc}, and FF, 0.87 $mAcm^{-2}$, 4.20 V, and 27.877 %. The PCE is dropped by 63.89 % for modules of active area 9.25 cm^2 and 88.68 % of modules of active area 63 cm^2. The PCE of the modules are decreased sharply due to loss in FF, and J_{sc} of the modules. These losses are exhibits due to quality of layer morphology, layer interfaces, and design of module. The PCE could be potentially improved up to the desired value by the further optimization of layer morphology, layer interfaces, design of module geometry, and film deposition/printing methods. The results referred that PTB7Th:$PC_{71}BM$ is a splendid structure for future organic solar modules due to its high performance and compatibility with large area coatings.

Keywords: Inverted organic solar cell, PTB7-Th:$PC_{71}BM$, Organic solar modules, Spin coating, Short circuit current, Fill factor

Dr. Belal Usmani Assistant Professor, Physics Dept., Shibli National College, Azamgarh _276001

1. Introduction

The fast development, industrial growth and extensive usage of electricity consuming devices across the globe demand energy reservoir. However, extensive utilization of energy causes depletion of natural resources and increase of global warming (Abdmouleh et al., 2015; Lior, 2008; Mekhilef et al., 2011; Schnitzer et al., 2007). Solar energy is one of the most potential renewable energy resources, which can be utilized by direct converting into electricity employing photovoltaic technology (Aman et al., 2015; Liu et al., 2013; Thirugnanasambandam et al., 2010; van der Staaij et al., 2021). Several photovoltaic technologies such as based on Silicon (Si), Cadmium Telluride (CdTe), and Copper Indium Gallium Selenide (CIGS) are competent to full fill the a significant fraction of this demand. However, these technologies showed hurdle due to high manufacturing process cost, manufacturing obstacle because of complex chemistry, and environmental concerns related to Cd in CdTe (Kessler and Rudmann, 2004; Kwak et al., 2020; Lee and Ebong, 2017; Polman et al., 2016; Ramanujam and Singh, 2017). Organic solar cells (OSCs) technologies comprising donor and acceptor type of organic semiconductors intermixed to form bulk-heterojunction (BHJ) have potential to become an alternative photovoltaic technology because of cost-effectiveness, light weight, mechanical flexibility, and have the competence to manufacture on the large area (Cheng et al., 2018, 2009; Clarke and Durrant, 2010; Hoppe and Sariciftci, 2004; Hou et al., 2018; Lee et al., 2015; Yao et al., 2016). There has been immense progress in BHJ organic solar cells. The PCE of BHJ organic solar cells has been reached up to 18 % (Liu et al., 2021) because of remarkable progress in donor/acceptor blend materials. However, these tremendous PCE of OSCs devices would be noted with laboratory scale area (> 1 mm^2). The transformation of laboratory scale area OSCs devices to large area modules with stability and without significant loss in PCE exhibits a number of challenges. Particularly, deposition of films accompanied by required morphologies over a large area, optimum designs of device structure, appropriate processing techniques (Kang et al., 2013; Lim et al., 2017; Tsai et al., 2015).

In the company of various blends employed in BHJ organic solar cells, those consist of Poly([2,6′-4,8-di(5-ethylhexylthienyl)benzo[1,2-*b*;3,3-*b*]dithiophene]{3-fluoro-2[(2ethylhexyl)carbonyl]thieno[3,4-*b*]thiophenediyl}) (PTB7-Th) donor materials blended along with [6,6]-phenyl C71-butyric acid methyl ester ($PC_{71}BM$) acceptor have demonstrated

magnificent PCE >10% (Kobori and Fukuda, 2017; Usmani et al., 2021; Wan et al., 2016). However, the PCE efficiency of these devices is reported for small scale device area. On the other hand these blend (PTB7-Th:$PC_{71}BM$) of BHJ OSCs is not more investigated for large area modules. Hong et al. demonstrated a new modules architecture for making large area modules of blend PTB7-Th:$PC_{71}BM$ BHJ OSCs and reported a high module efficiency 7.5% with area of 4.15 cm^2 (Hong et al., 2016). Barreiro-Arguelles et al. investigated the OSCs modules performance and stability with blend PTB7:$PC_{71}BM$ as photoactive layer (Barreiro-Argüelles et al., 2018). In this work, we extended our study of lab scale optimized OSCs devices (0.06 cm^2 & PCE of 9.0%) with inverted structure ITO/ZnO/ PTB7-Th:$PC_{71}BM$/MoO_3/Ag to large area modules (Usmani et al., 2021). The organic solar modules based on blend PTB7-Th:$PC_{71}BM$ are fabricated employing spin coating techniques. The OPV modules comprising 5 Cells and 10 cells connected in series possessing total active area 9.25 cm^2, and 63 cm^2 showed the PCE of 3.256%, & 1.019%, which in future could be further improved by optimizing layer morphology & interface, and processing techniques. The study stimulate that the OPV modules based on PTB7-Th:$PC_{71}BM$ blend may be a promising candidate for the large area OSCs applications.

2. Experimental section

2.1 Materials

ITO coated glass substrates with a sheet resistance of 14Ω/sq were purchased from Lumtec, Taiwan. Zinc acetate (99.99%), 2-methoxyethanol (99.8%), and ethanolamine (99.0%) were purchased from Sigma Aldrich. Poly([2,6′-4,8-di(5-ethylhexylthienyl)benzo[1,2-*b*;3,3*b*]dithiophene]{3-fluoro-2[(2ethylhexyl)carbonyl]thieno[3,4-*b*]thiophenediyl}) (PTB7-Th) and [6,6]-phenyl C71-butyric acid methyl ester ($PC_{71}BM$) ($PC_{71}BM$) were purchased from 1Materials, Canada. 1,8-Diiodooctane was purchased from Sigma-Aldrich. Chlorobenzene used as solvent in device fabrication process was purchased from Alfa Aesar. All these commercially available materials were used as received without further purification.

2.2 Modules design, fabrication, & characterization

Schematic of inverted ITO/ZnO/PTB7-Th:$BC_{71}BM$/MoO_3/Ag OSC device structure and energy band diagram shown in figure 1 (a & b), which is followed for the fabrication of OPV modules. Inverted structure of OPV modules are fabricated on 5cm x 5cm & 11cm x 11cm ITO coated glass substrate. Schematic representation of cross-sectional view as well as designs parameters of the 5cm x 5cm OPV module shown in figure 2 (a & b), it comprises 5 cells connected in series. Each cell has included the size of 5cm in width and 3.7 cm in length and each cell is parted by 0.1 cm space. The total active area is 9.25cm^2. The OPV module is designed in series to obtain the output voltage. In a series circuitry, each cell should be worked properly to complete the circuit of the module. Hereof, to get the maximum performance of the module film and interface uniformity of each cell is very important. Figure 2 (c) showed the photograph of 5cm x 5cm OPV module. Schematic representation of cross-sectional view as well as designs parameters of the 11cm x 11cm OPV module shown in figure 3 (a & b), it comprises 10 cells connected in series. One cell of the 10 cell have size of 0.9cm in width and 10cm in length and other 9 cell comprises with size of 0.6cm in width and 10cm in length and each cell is parted by 0.1cm space. The total active area is 63cm^2. Figure 3 (c & d) showed the photograph of 11cm x 11cm OPV module and metal mask for making interconnection, respectively. These designed are selected to perform the study of the given device structure (Figure 1(a)) with active layer PTB7Th:$PC_{71}BM$. However, for the commercial application purpose need to rethink for the design to get the maximum active area and performance of the module.

5 cm x 5 cm and 10 cm x 10 cm pieces of ITO coated glass substrate were cut from a large piece of substrate. First, ITO coated glass substrates were patterned using photolithography technique. The patterned substrates were ultrasonically cleaned in a boiled soap solution for 10 min, followed by rinsing and ultrasonication in DI water, acetone, and isopropyl alcohol (IPA) for 10 min, respectively, followed by drying with nitrogen. Patterned substrates were UV Ozone (UVO) treated for ~20 min. For the preparation of ZnO films appropriate solutions were spin coated onto patterned ITO coated UVO treated glass substrates for 60s at 2000 rpm followed by thermal annealing at 250°C for 10 min. Organic photoactive layer solution was prepared by dissolving PTB7-Th (10 mg) and PC71BM (15 mg) in chlorobenzene (970µl) and 1,8Diiodooctance (30 µl). The solution was stirred at room temperature for 8h and then filtered using 0.22µm polytetrafluoroethylene (PTFE) filter. The deposition of active layer onto ZnO/ITO/glass substrate was performed by spin coating the solution at 2000 rpm for 15 sec (for the module size: 5 cm x 5 cm) and 800 rpm for

15sec (for the module size: 11 cm x 11 cm) followed by thermal treatment on a hot plate at 40C for 2 h in nitrogen glove box. Finally, MoO_3 film of 10 nm thickness to act as hole transporting layer (HTL) and Ag layer of 100 nm thickness as top metal electrode were thermally evaporated under high vacuum, respectively. The estimated active area of devices as defined by the overlap of the anode and cathode was 9.25 cm^2 and 63 cm^2. The current (I) –Voltage (V) characteristics of the OPV modules were measured in air using TriSol™ concentrated photovoltaic (CPV) solar simulator in dark as well as under one sun illumination (simulated solar radiation of AM 1.5G spectrum).

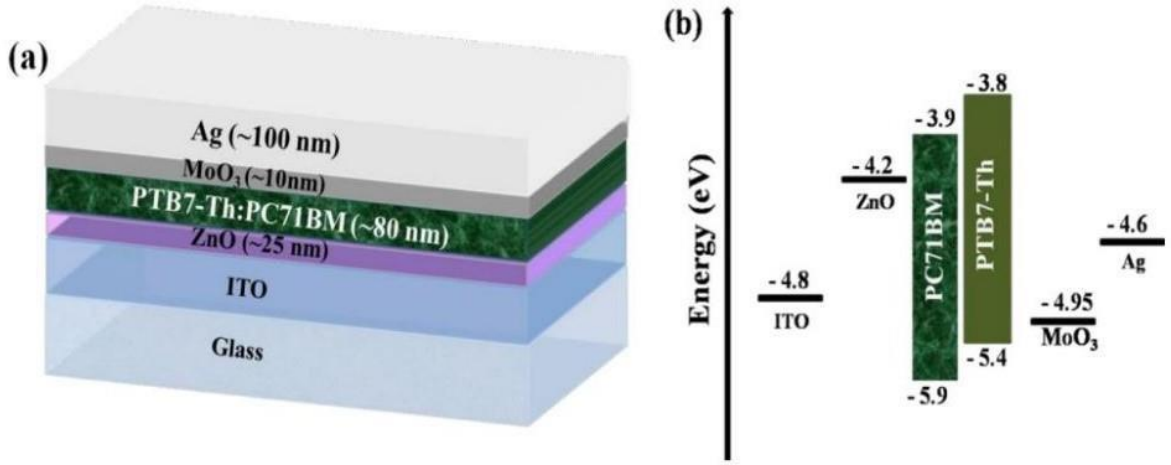

Fig. 1. (a) Schematic of inverted ITO/ZnO/PTB7-Th:$BC_{71}BM$/MoO_3/Ag bulk hetrojunction OSC Device. (b) Energy band diagram of bulk hetrojunction OSC Device.

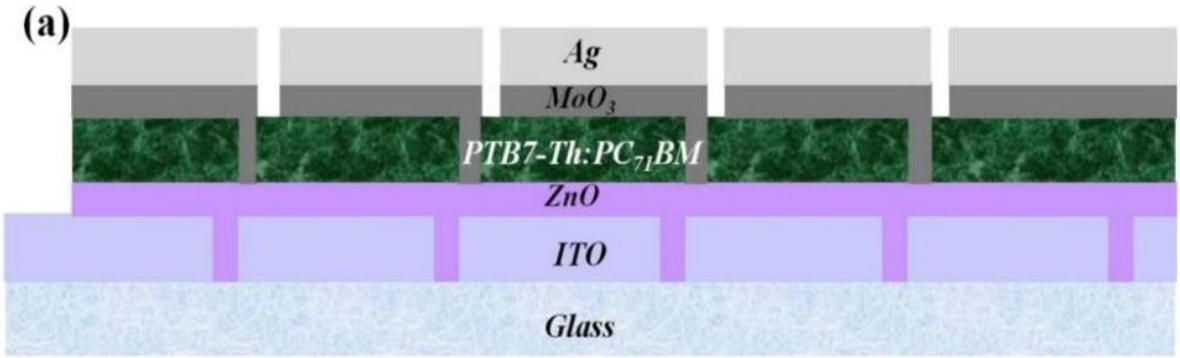

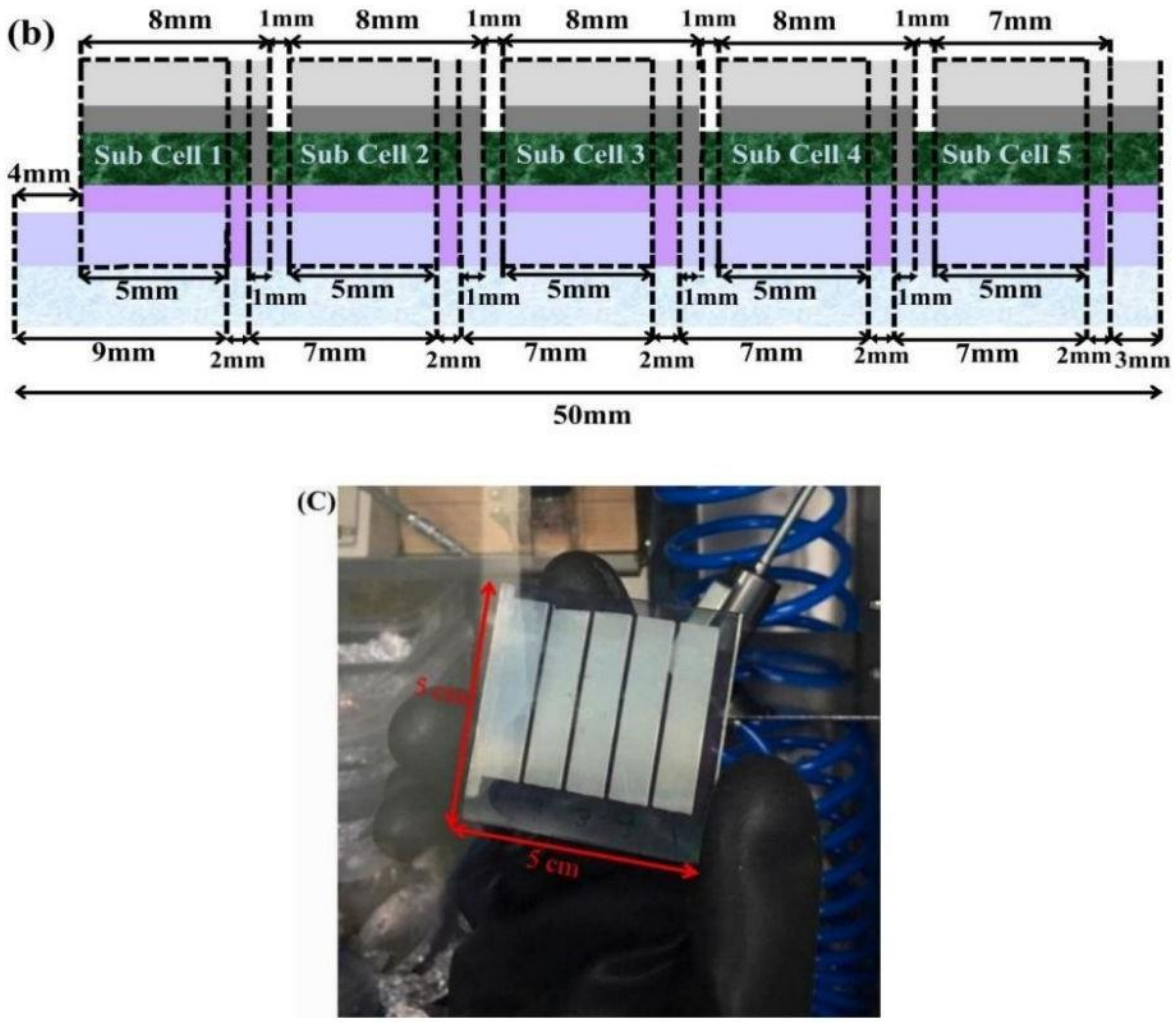

Fig. 2. **(a)** Schematic illustration of cross-sectional view of series-connected 5 cell of inverted OPV module (Module size: 5cm x 5cm). **(b)** Schematic representation of the module with length, width, & spaced parameters. **(c)** Photographs of 5cm x 5cm module.

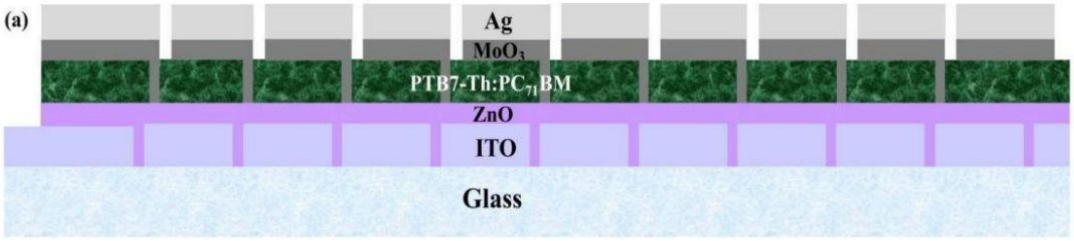

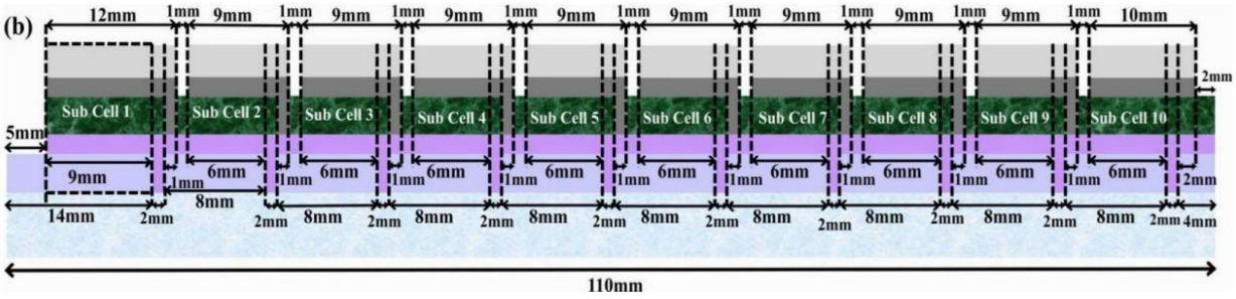

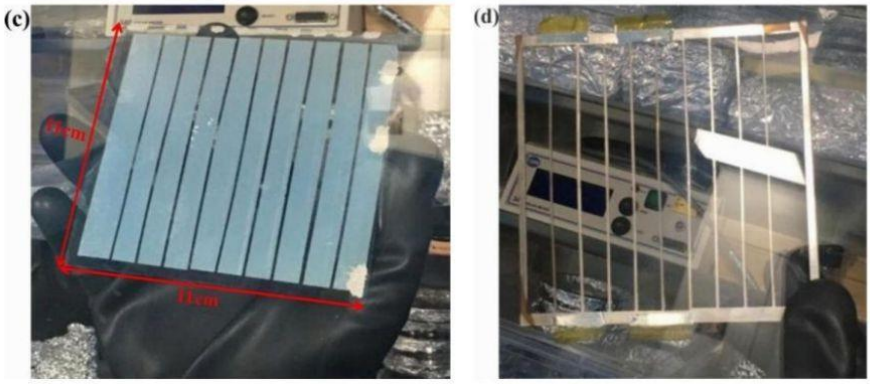

Fig. 3. **(a)** Schematic illustration of cross-sectional view of series-connected 10 cell of inverted OPV module (Module size: 11cm x 11cm). **(b)** Schematic representation of the module with length, width, & spaced parameters. **(c)** Photographs of 5cm x 5cm module. **(d)** Metal mask for making interconnection.

3. Results and discussion

The performance of OPV modules is affected by several factors such as high series resistance, effect of defective cells, & aperture ratio (Ã et al., 2009). To examine the performance of organic photovoltaic (OPV) modules, we fabricated inverted structured modules with configuration Glass/ITO/ZnO/PTB7-Th:$PC_{71}BM$/MoO_3/Ag with device structure and energy band diagram (Usmani et al., 2021) shown in Fig. 1(a -b). The photovoltaic performance of OPV modules with two deferent active area 9.25 cm^2 and 63 cm^2 comprising total area 25 cm^2 and 144 cm^2, under illumination of AM 1.5G, 100 $mW.cm^{-2}$ and under dark is shown in Figure 4 (a-b). The photovoltaic performance of OPV modules with varying active area is summarized in Table 1. OPV modules with active area 9.25 cm^2 are characterized by the following average photovoltaic performance parameters (from three samples): short-circuit current density (J_{sc}) of 2.88 mA/cm^2, open circuit voltage (V_{oc}) of 2.85 V, fill factor (FF) of 0.30 and power conversion efficiency (PCE) of 2.53%. The OPV module with active area 63 cm^2 shows short-circuit current density (J_{sc}) of 0.87 mA/cm^2, an open-circuit voltage (V_{oc}) of 4.2 V and a fill factor (FF) of 0.27, leading to PCE of 1.01%. As we observed (Table 1) that the average photovoltaic performance of small active area (0.06 cm^2) devices are comparable to the PTB7-Th:$PC_{71}BM$ blend based organic photovoltaic devices (Usmani et al., 2021). However, when the active area scaled up ~ 154 times (to 9.25cm^2) and 1050 times (to 63 cm^2), there is notable decrease in the PCE of OPV modules leading to an average value of 2.53 % and 1.01% (table 1). These values are approximately 27% (for 9.25cm^2) and 10% (for 9.25cm^2) of PCE value corresponding to devices with 0.06cm^2 active area (Figure 5b). In the same way, the values of J_{sc} were reduced approximately 15% & 4% (Figure 5a), and FF values approximately 49%, and 45%, respectively (Figure 5b). The deficiency in PCE of OPV module with large active area is mainly concerned to the decrease in FF and J_{sc}. The main reason in reduction of FF with increasing active area of the OPV modules is effective contribution of series resistance from ITO (Jeong et al., 2011; Xiao et al., 2016). However, The losses in current density (J_{sc}) is attributed to non-uniformity in morphology and thickness of the OPV modules with large area (Agrawal et al., 2016; Jeong et al., 2011). V_{oc} is not the function of active area of the devices. The V_{oc} of the OPV module is the addition of the subcells V_{oc}. On the contrary, the V_{oc} values of the increased number of subcells showed less advancement (Table 1 & Figure 5(a)). The values of V_{oc} is related to the junction properties of the donor and acceptor layers, and work function of

cathode and anodes (Brabec et al., 2002; Cheyns et al., 2008; Mihailetchi et al., 2012). The present study noticed that controlling the series resistance, uniformity in morphology and thickness across the entire active area is crucial to retain the higher efficiency demonstrated by small area devices.

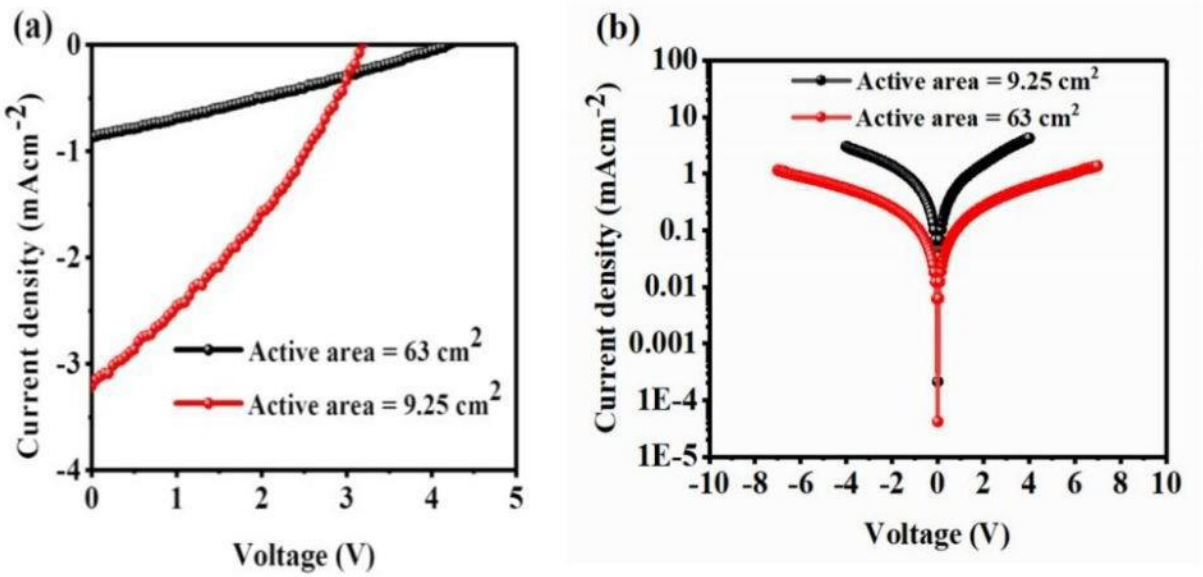

Fig. 4. (a) *J-V* curves of OSMs based on ITO/ZnO/PTB7-Th:$PC_{71}BM$/MoO_3/Ag inverted structure with active area 9.25 cm^2 and 63 cm^2 under illumination of AM 1.5G, 100 mW cm^{-2}. **(b)** *J-V* characteristics curve of OSMs under dark condition.

Table 1

Photovoltaic performance of OSCs devices based on ITO/ZnO/PTB7Th:$PC_{71}BM$/MoO_3/Ag structure with varying active area under the illumination of AM1.5G, 100 mWcm^2. Numbers in parenthesis represent the average value of 6 tested devices for 0.06 cm^2, 3 tested devices for 9.25 cm^2, and one device for 63 cm^2. The values out of the parenthesis represent the device with the best performance.

Active Area (cm^2)	V_{oc} (V)	J_{sc} ($mAcm^{-2}$)	FF (%)	PCE (%)	R_s (Ω-cm^2)	R_{sh} (Ωcm^2)	Ref.
0.06	0.801	19.3 (19.0±0.2)	61.8 (61.0±0.9)	9.55 (9.31±0.28)	8.3	333.3	[27]
9.25	3.20 (2.85±0.312)	3.210 (2.886±0.359)	31.719 (30.48±1.081)	3.256 (2.531±0.641)	57.870	88.967	
63	4.2	0.87	27.877	1.019	32.594	62.35	

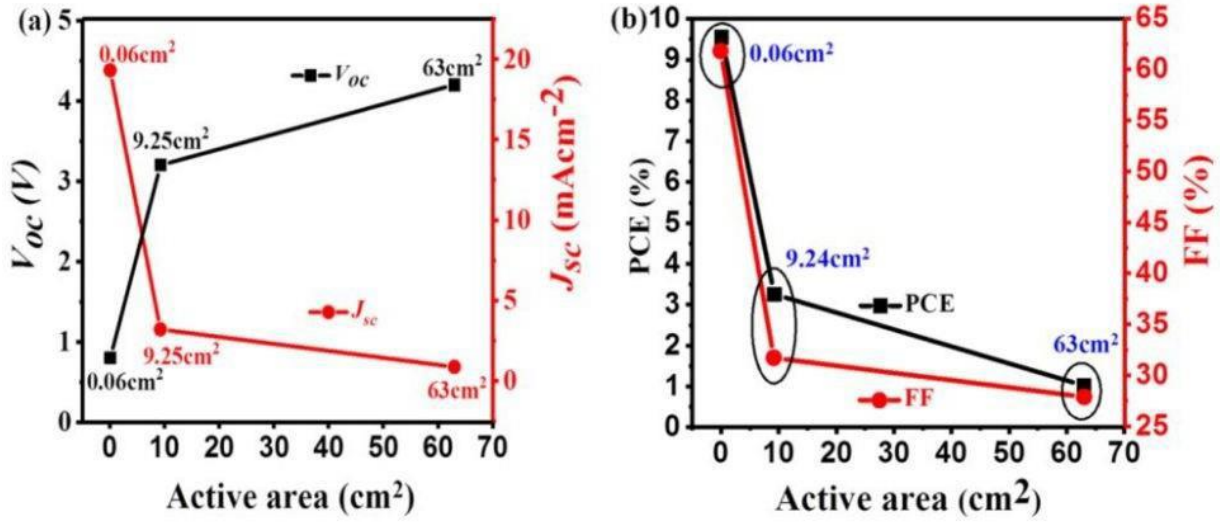

Fig. 5. (a) V_{oc} and J_{sc} curve with variation of active area**. (b)** PCE and FF curve with variation of active area.

4. Conclusions

In conclusion, the photovoltaic performance of PTB7-Th:$PC_{71}BM$ based large area OPV modules were studies when the active area is scaled from 0.06 cm^2 to 9.25 cm^2 and 63 cm^2. PCE of the 5-cell and 10-cell modules were 2.53% and 1.01% with active area 9.25 cm^2 and 63 cm^2. These values were 27% and 10% of PCE value corresponding to devices with 0.06 cm^2 active area. the present study noticed that controlling the series resistance, uniformity in morphology and thickness across the entire active area is crucial to retain the higher efficiency demonstrated by small area devices. However, it is possible to improve fabrication conditions and reduce series resistance from ITO to get the better performance from PTB7-Th:$PC_{71}BM$ based OPV modules.

Acknowledgments

Authors thank Department of Science and Technology for funding through India-UK APEX-II project, Newton Prize Funds, and EPSRC (UK) for funding through SUNRISE under GCRF call.

References

Ã, R.T., Bernkopf, J., Jia, S., Krieg, J., Li, S., Storch, M., Laird, D., 2009. Solar Energy Materials & Solar Cells Large-area organic photovoltaic module — Fabrication and performance 93, 442–446. https://doi.org/10.1016/j.solmat.2008.11.018

Abdmouleh, Z., Alammari, R.A.M., Gastli, A., 2015. Review of policies encouraging renewable energy integration & best practices. Renew. Sustain. Energy Rev. 45, 249–262. https://doi.org/10.1016/j.rser.2015.01.035

Agrawal, N., Zubair, M., Majumdar, A., Gahlot, R., Khare, N., 2016. Solar Energy Materials & Solar Cells Ef fi cient up-scaling of organic solar cells 157, 960–965. https://doi.org/10.1016/j.solmat.2016.07.040

Aman, M.M., Solangi, K.H., Hossain, M.S., Badarudin, A., Jasmon, G.B., Mokhlis, H., Bakar, A.H.A., Kazi, S.N., 2015. A review of Safety, Health and Environmental (SHE) issues of solar energy system. Renew. Sustain. Energy Rev. 41, 1190–1204. https://doi.org/10.1016/j.rser.2014.08.086

Barreiro-Argüelles, D., Ramos-Ortiz, G., Maldonado, J.L., Pérez-Gutiérrez, E., Romero-Borja, D., Meneses-Nava, M.A., Nolasco, J.C., 2018. Stability study in organic solar cells based on PTB7:PC71BM and the scaling effect of the active layer. Sol. Energy 163, 510–518. https://doi.org/10.1016/j.solener.2018.01.090

Brabec, C.J., Cravino, A., Meissner, D., Sariciftci, N.S., Rispens, M.T., Sanchez, L., Universitat, J.K., 2002. The influence of materials work function on the open circuit voltage of plastic solar cells 404, 368–372.

Cheng, P., Li, G., Zhan, X., Yang, Y., 2018. Next-generation organic photovoltaics based on non-fullerene acceptors /639/301/299/946 /639/624/399 review-article. Nat. Photonics 12, 131–142. https://doi.org/10.1038/s41566-018-0104-9

Cheng, Y.-J., Yang, S.-H., Hsu, C.-S., 2009. Cr900182S.Pdf. Chem. Rev. 109, 5868–5923.

Cheyns, D., Poortmans, J., Heremans, P., Deibel, C., Verlaak, S., Rand, B.P., Genoe, J., 2008. Analytical model for the open-circuit voltage and its associated resistance in organic planar heterojunction solar cells 1–10. https://doi.org/10.1103/PhysRevB.77.165332

Clarke, T.M., Durrant, J.R., 2010. Charge photogeneration in organic solar cells. Chem. Rev. 110, 6736–6767. https://doi.org/10.1021/cr900271s

Hong, S., Kang, H., Kim, G., Lee, S., Kim, S., Lee, J.H., Lee, J., Yi, M., Kim, J., Back, H., Kim, J.R., Lee, K., 2016. A series connection architecture for large-area organic photovoltaic modules with a 7.5% module efficiency. Nat. Commun. 7. https://doi.org/10.1038/ncomms10279

Hoppe, H., Sariciftci, N.S., 2004. Organic solar cells: An overview. J. Mater. Res. 19, 1924– 1945. https://doi.org/10.1557/JMR.2004.0252

Hou, J., Inganas, O., Friend, R.H., Gao, F., 2018. Organic solar cells based on non-fullerene acceptors. Nat. Mater. 17, 119–128. https://doi.org/10.1038/NMAT5063

Jeong, W., Lee, J., Park, S., Kang, J., Kim, J., 2011. Reduction of Collection Effi ciency of Charge Carriers with Increasing Cell Size in Polymer Bulk Heterojunction Solar Cells 343– 347. https://doi.org/10.1002/adfm.201001578

Kang, N.S., Ju, B.K., Yu, J.W., 2013. Module structure for an organic photovoltaic device. Sol. Energy Mater. Sol. Cells 116, 219–223. https://doi.org/10.1016/j.solmat.2013.05.009

Kessler, F., Rudmann, D., 2004. Technological aspects of flexible CIGS solar cells and modules. Sol. Energy 77, 685–695. https://doi.org/10.1016/j.solener.2004.04.010

Kobori, T., Fukuda, T., 2017. Effect of optical intensity distribution on device performances of PTB7-Th : PC 71 BM-based organic photovoltaic cells. Org. Electron. 51, 76–85. https://doi.org/10.1016/j.orgel.2017.09.006

Kwak, J. Il, Nam, S.H., Kim, L., An, Y.J., 2020. Potential environmental risk of solar cells: Current knowledge and future challenges. J. Hazard. Mater. 392, 122297. https://doi.org/10.1016/j.jhazmat.2020.122297

Lee, C., Kang, H., Lee, W., Kim, T., Kim, K.H., Woo, H.Y., Wang, C., Kim, B.J., 2015. Highperformance all-polymer solar cells via side-chain engineering of the polymer acceptor: The importance of the polymer packing structure and the nanoscale blend morphology. Adv. Mater. 27, 2466–2471. https://doi.org/10.1002/adma.201405226

Lee, T.D., Ebong, A.U., 2017. A review of thin film solar cell technologies and challenges. Renew. Sustain. Energy Rev. 70, 1286–1297. https://doi.org/10.1016/j.rser.2016.12.028 Lim, S.L., Ong, K.H., Li, J., Yang, L., Chang, Y.F., Meng, H.F., Wang, X., Chen, Z.K., 2017. Efficient, large area organic photovoltaic modules with active layers processed with nonhalogenated solvents in air. Org. Electron. 43, 55–63. https://doi.org/10.1016/j.orgel.2017.01.001

Lior, N., 2008. Energy resources and use: The present situation and possible paths to the future. Energy 33, 842–857. https://doi.org/10.1016/j.energy.2007.09.009

Liu, F., Zhou, L., Liu, Wenrui, Zhou, Z., Yue, Q., Zheng, W., Sun, R., Liu, Wuyue, Xu, S., Fan, H., Feng, L., Yi, Y., Zhang, W., Zhu, X., 2021. Organic Solar Cells with 18% Efficiency Enabled by an Alloy Acceptor: A Two-in-One Strategy. Adv. Mater. 33, 1–8. https://doi.org/10.1002/adma.202100830

Liu, S.-Y., Perng, Y.-H., Ho, Y.-F., 2013. The effect of renewable energy application on Taiwan buildings: What are the challenges and strategies for solar energy exploitation? Renew. Sustain. Energy Rev. 28, 92–106. https://doi.org/10.1016/j.rser.2013.07.018